probability is only 0.6. If the reactivity at the surface were infinite, then the yields surface and solvent reaction products would be 40% and 60%, respectively. Stated another way, an octyl radical in DEE at a distance 17 000 Å from a perfectly reactive surface has only a 60% "escape" probability.

Actually, no surface can be perfectly reactive. We now derive the probability A_r that a radical at a distance r from a less than perfectly reactive surface will react at the surface instead of reacting with the solvent. We use a modified version of Noyes' molecular-pair method.[33]

Let an "encounter" with the reactive surface begin when a radical diffuses to the surface. Let it end when the radical thereafter first reaches an arbitrarily chosen distance l from the surface (Figure 4) or when the radical reacts, either at the surface or with the solvent, before reaching the distance l. Let α and ϵ, respectively, be the probabilities of surface and solvent reactions during an encounter. Then the probability that a radical will escape intact from an encounter is $1 - (\alpha + \epsilon)$.

Since radicals at distances r and l from the surface have probabilities ϕ_r and ϕ_l of surviving until they reach the surface for the first time, the total probability A_r of the surface reaction is given by eq A3 and A4. If ϵ is much smaller than $1 - \alpha$, which

$$A_r = \phi_r\alpha + \phi_r(1 - \alpha - \epsilon)\phi_l\alpha + \phi_r(1 - \alpha - \epsilon)\phi_l(1 - \alpha - \epsilon)\phi_l\alpha + \ldots \quad \text{(A3)}$$

$$A_r = \alpha\phi_r/[1 - (1 - \alpha - \epsilon)\phi_l] \quad \text{(A4)}$$

will be the case for all except the largest possible k_S and α values, then it can be neglected. Since l is arbitrary, we can let it be small. As l becomes small, so does α, but the ratio α/l may approach a finite limiting value. At the same time, ϕ_l approaches $1 - l/\sigma$. Then A_r is given by eq A5, where δ is the limit of α/l as $l \to 0$.

$$A_r = \delta\sigma\phi_r/(1 + \delta\sigma) \qquad (\text{if } \alpha \to 0 \text{ and } \alpha/l \to \delta \text{ as } l \to 0) \quad \text{(A5)}$$

The same equation can be derived through a diffusion-equation treatment in which δ is the proportionality constant of the radiation boundary condition (see Appendix of the preceding paper, eq A5-A7 there).[1,4,17]

For Grignard reagent formation from primary alkyl halides in solvents such as DEE and THF, δ appears to be $\sim 10^{-2}$ Å^{-1} (see above). If σ is 17 000 Å, then $\delta\sigma$ is 170 and $1 + \delta\sigma$ is 171, so that A_r is $(170/171)\phi_r$. Thus, a radical in DEE that is initially 17 000 Å from the surface has very nearly the same probability, 0.4, of reacting at the surface instead of with the solvent whether the surface approaches perfect reactivity (δ approaching infinity) or considerably less ($\delta = 10^{-2}$ Å^{-1}).

On reflection, the reason is clear: a δ value of 10^{-2} Å^{-1} is large enough to guarantee that nearly every radical that reaches the surface reacts there instead of with the solvent. In eq A5, the factor $\delta\sigma/(1 + \delta\sigma)$ is the probability A_0 that a freely diffusing radical that is initially at the surface will react with the surface instead of the solvent. As long as δ and σ are such that A_0 is near unity, then A_r will be nearly the same for all values of δ, namely, ϕ_r.

For a radical that is initially at the surface to have a 50% probability of escaping surface reaction, $\delta\sigma$ must be unity. If δ is 10^{-2} Å^{-1}, then k_S has to be 3×10^7 s^{-1}, $\sim$30 000 times the actual values of k_S for primary alkyl radicals in DEE at 22 °C. Alternatively, if k_S is 1×10^3 s^{-1}, then δ has to be $1/\sigma$ or 6×10^{-5} Å^{-1}, $\sim 1/170$th of that found.

Thus, freely diffusing radicals formed at a sufficiently reactive surface will undergo surface reaction instead of reaction with solvent, even though their diffusive excursions may take them many, even thousands of, Ångstrom units away from the surface.

Registry No. Mg, 7439-95-4; 5-hexenyl bromide, 2695-47-8.

(33) (a) Noyes, R. M. *J. Chem. Phys.* **1954**, *22*, 1349-1359. (b) Noyes, R. M. *Prog. React. Kinet.* **1961**, *1*, 129-160.

Organoiodinane Reagents for Phosphate Cleavage: Experimental and Computational Studies†

Robert A. Moss,* Bogusława Wilk, Karsten Krogh-Jespersen,* John T. Blair, and John D. Westbrook

Contribution from the Wright and Rieman Laboratories, Department of Chemistry, Rutgers, The State University of New Jersey, New Brunswick, New Jersey 08903. *Received June 3, 1988*

Abstract: Several analogues of 1-oxido-1,2-benziodoxol-3(1*H*)-one, **1** (the valence tautomer of *o*-iodosobenzoate), were examined for their ability to cleave *p*-nitrophenyl diphenyl phosphate in aqueous micellar cetyltrimethylammonium chloride at pH 8. These included the 5,5-dimethyl (**7**) and 5,5-bis(trifluoromethyl) (**8**) analogues, as well as the parent 1-oxidoiodoxol-(3*H*)-ones **9** and **10**. The kinetic reactivity order was **1** > **9** > **10** > **8** ≫ **7**. The results are discussed in terms of the relative acidities shown by the I–OH forms of the catalysts and the nucleophilicities of their I–O$^-$ conjugate bases. Ab initio molecular orbital calculations were performed on **10**, its conjugate acid (**10**-OH), the desoxo analogues (**11**, **11**-OH), and their dimethyl (**12**, **12**-OH) and bis(trifluoromethyl) (**13**, **13**-OH) derivatives to aid this analysis. The electronic structures of these species are discussed in detail.

o-Iodosobenzoate, in its preferred, valence tautomeric, 1-oxido-1,2-benziodoxol-3(1*H*)-one form (**1**), is a potent α-effect O-nucleophile.[1] When solubilized in cationic micellar solution, **1** and its simple derivatives prove to be excellent catalysts for the cleavage of reactive, toxic phosphates.[2-4] More recently, the catalytic properties of **1** have been studied in microemulsions[5] and in nematic lyotropic liquid crystals.[6]

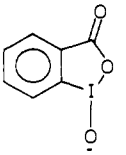

1

A natural extension of this work involves the examination of close relatives of **1**, in an attempt to find an even more potent

† Dedicated to the memory of Professor Emil Thomas Kaiser.

0002-7863/89/1511-0250$01.50/0

Chart I

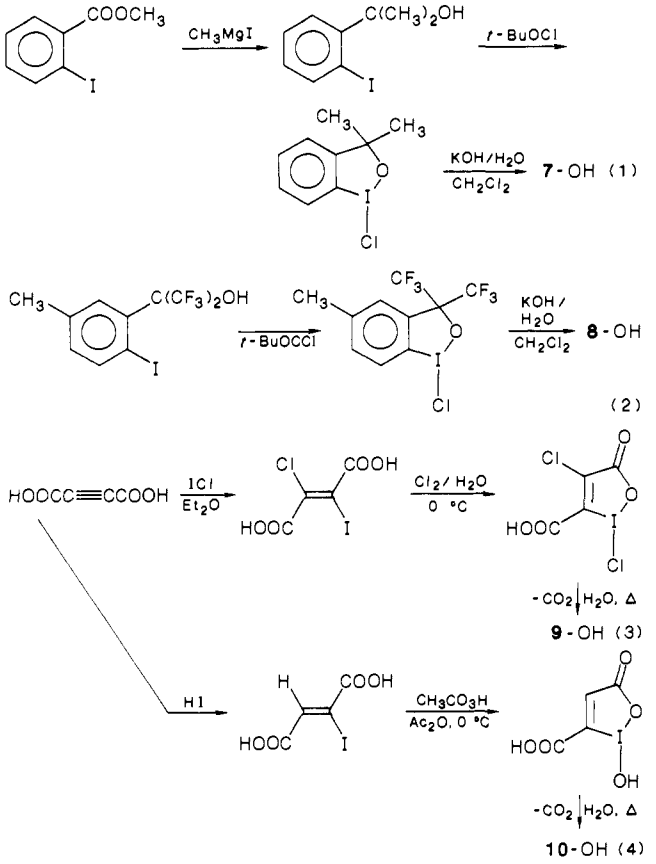

nucleophile. Accordingly, iodoxybenzoate reagents have been surveyed,[7] while in our laboratory, a series of organoiodinane oxyanions (**2**–**6**) was tested.[8] Interestingly, none of these reagents,

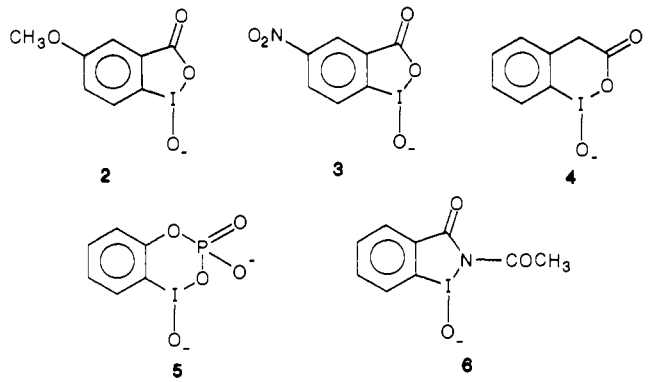

2 **3** **4**

5 **6**

where substituents (**2** and **3**), ring size (**4**), or heteroatoms (**5** and **6**) were varied, proved superior to **1** as a catalyst for cleavage of the test substrate, *p*-nitrophenyl diphenyl phosphate (PNPDPP).[8]

$(PhO)_2P(O)OC_6H_4NO_2$

PNPDPP

Indeed, **2** and **3** were marginally and **4**–**6** markedly inferior to **1** by kinetic criteria under comparable conditions. The iodoxybenzoate analogues of **1**, however, were kinetically comparable in their reactivities toward PNPDPP and a phosphinate substrate.[7]

In the present study, we extend our survey of iodosobenzoate analogues, considering organoiodinane oxyanions **7**–**10**. In **7**, the lactone carbonyl of **1** is replaced by the saturated, electron-do-

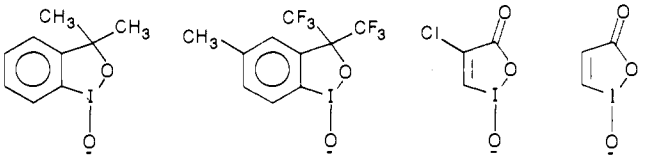

7 **8** **9** **10**

nating *gem*-dimethyl unit, whereas in **8** the electron-withdrawing *gem*-bis(trifluoromethyl) groups simulate the original carbonyl moiety of **1** (although they lack its trigonal ring carbon atom). Reagents **9** and **10** lack the benzo substituent of **1**, but retain the essential iodoxolone heterocycle; indeed **10** can be considered the "parent" of **1**.

In addition to the experimental studies, we have carried out ab initio calculations on **10**, its conjugate acid (**10**-OH), and on their desoxo analogues **11** and **11**-OH. The fully optimized structures of the latter, together with standard CH_3 and CF_3 bond lengths and angles, were used to generate calculated structures for **12** and **13** and their conjugate acids. Taken together, these

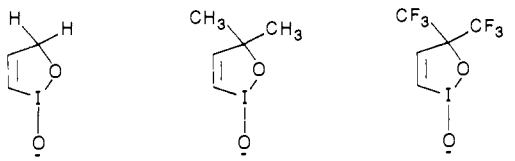

11 **12** **13**

theoretical calculations add to our understanding of structure and bonding in the iodoxolones and iodoxols. Additionally, the calculated relative energy changes that accompany ionizations of **10**-OH–**13**-OH can be correlated with experimental pK_a data for the conjugate acids of **1**, **7**, **8**, and **10**. The ease of conversion of these I–OH acids to their nucleophilic I–O^- conjugate bases, together with the intrinsic nucleophilicity of the latter, are fundamental to their catalytic properties.

Results

Synthesis. Preparations of the iodinane reagents **7**-OH–**10**-OH are outlined in Chart I. Reagent **7**-OH was prepared by the method of Amey and Martin;[9] cf. Chart I, eq 1. Methyl *o*-iodobenzoate was converted (73%) to the aryldimethylcarbinol with methyl Grignard,[10] the crude carbinol was cyclized to the chloroiodinane (57%) with *tert*-butyl hypochlorite,[9] and the desired **7**-OH was obtained in 54% yield by hydrolysis with aqueous KOH.[9] The final product had appropriate melting point, NMR spectrum, and elemental analysis and was homogeneous on TLC and gave 99% oxidative activity upon $KI/Na_2S_2O_3$ iodometric titration.[11]

The preparation of the (*o*-iodophenyl)bis(trifluoromethyl)-carbinol (Chart I, eq 2) from *p*-toluidine and its *tert*-butyl hypochlorite cyclization to the bis(trifluoromethyl)chlorobenziodoxol have been described.[9] The chloroiodinane was purified by sublimation[9] and then hydrolyzed to **8**-OH in a two-phase, aqueous KOH/CH_2Cl_2 system, with benzyltriethylammonium chloride as a phase-transfer catalyst. Reagent **8**-OH was obtained in 75% yield after chromatography on silica gel and was characterized by ^1H NMR spectroscopy, elemental analysis, and iodometric titration[11] (99.3% activity).

(1) Moss, R. A.; Swarup, S.; Ganguli, S. *J. Chem. Soc., Chem. Commun.* **1987**, 860.
(2) Moss, R. A.; Alwis, K. W.; Bizzigotti, G. O. *J. Am. Chem. Soc.* **1983**, *105*, 681.
(3) Moss, R. A.; Alwis, K. W.; Shin, J.-S. *J. Am. Chem. Soc.* **1984**, *106*, 2651.
(4) Moss, R. A.; Kim, K. Y.; Swarup, S. *J. Am. Chem. Soc.* **1986**, *108*, 788.
(5) Mackay, R. A.; Longo, F. R.; Knier, B. L.; Durst, H. D. *J. Phys. Chem.* **1987**, *91*, 861.
(6) Ramesh, V.; Labes, M. M. *J. Am. Chem. Soc.* **1988**, *110*, 739.
(7) Katritzky, A. R.; Duell, B. L.; Dursi, H. D.; Knier, B. *Tetrahedron Lett.* **1987**, *28*, 3899.
(8) Moss, R. A.; Chatterjee, S.; Wilk, B. *J. Org. Chem.* **1986**, *51*, 4303.
(9) Amey, R. L.; Martin, J. C. *J. Org. Chem.* **1979**, *44*, 1779.
(10) Brown, H. C.; Okamoto, Y.; Ham, G. *J. Am. Chem. Soc.* **1957**, *79*, 1906.
(11) Lucas, H. J.; Kennedy, E. R. In *Organic Syntheses*; Horning, E. C., Ed.; Wiley: New York, 1955 Collect. Vol. III, 482–484.

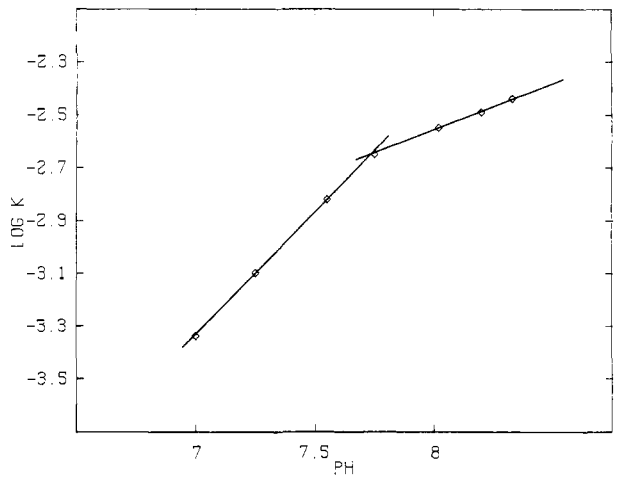

Figure 1. pH–rate profile for the cleavage of 1×10^{-5} M PNPDPP by 1×10^{-4} M **8**-OH in 1×10^{-3} M CTACl; log k_ψ vs pH. The discontinuity at pH 7.75 is taken as the systemic pK_a of **8**-OH.

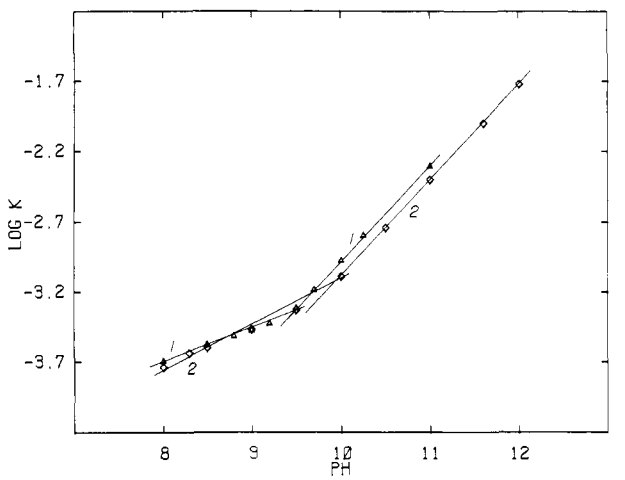

Figure 2. pH–rate profile for the cleavage of 1×10^{-5} M PNPDPP by 1×10^{-4} M **7**-OH in 1×10^{-3} M CTACl (line 1, △) and in CTACl alone (line 2, ◇). See text for discussion.

The 4-chloroiodoxolone **9**-OH was prepared by Thiele's method;[12,13] cf. Chart I, eq 3. Treatment of ethereal acetylenedicarboxylic acid with ICl gave *E*-α-chloro-β-iodofumaric acid,[12] isolated in 53% yield after extensive purification (see the Experimental Section). Chlorination[13] afforded the carboxychloroiodinane (70%), which decarboxylated and hydrolyzed to **9**-OH in boiling water. The final product was obtained in 72% yield after recrystallization from hot water and was characterized by melting point, IR, ^{1}H and ^{13}C NMR spectroscopy, elemental analysis, and iodometric titration[11] (99.6% activity).

Finally, addition of HI to acetylenedicarboxylic acid afforded, after purification, 82% of α-iodofumaric acid;[12] Chart I, eq 4. Reaction with 30% peracetic acid in acetic anhydride brought about both oxidation at iodine and cyclization, yielding 60% of the carboxyiodoxolone. This decarboxylated to **10**-OH (72%) in boiling water. Reagent **10**-OH was characterized by IR and ^{1}H NMR spectroscopy, elemental analysis, and iodometric titration[11] (99% activity).

pK_a Determinations. The reactive oxyanion forms of our iodinane reagents are shown in structures **1** and **7–10**. The pK_a of *o*-iodosobenzoic acid (**1**-OH) has been determined to be 7.25 from a pH–rate constant profile for the cleavage of *p*-nitrophenyl acetate in 0.02 M micellar cetyltrimethylammonium chloride (CTACl).[2] A similar method has now been used to determine the pK_a values of **8**-OH–**10**-OH.

In Figure 1, we present a pH–rate constant profile for the cleavages of 1×10^{-5} M PNPDPP by 1×10^{-4} M **8**-OH in 1×10^{-3} M micellar CTACl and 0.02 M aqueous phosphate buffer, μ = 0.08 (NaCl), at 25 ± 0.5 °C. These solutions also contained 1.0 vol % DMF and 0.33 vol % CH_3CN as consequences of reagent and substrate stock solution additions. Pseudo-first-order rate constants were spectrophotometrically determined by following the release of *p*-nitrophenoxide ion ($PNPO^-$) at 400 nm at 7 pH values between 7.0 and 8.33. The plot of log k_ψ vs pH (Figure 1) gave a discontinuity at pH 7.75, which was taken as the systemic pK_a of **8**-OH under our reaction conditions.

Systemic pK_a values were similarly determined as 7.45 for **9**-OH and 7.78 for **10**-OH in 1×10^{-3} M and 3×10^{-3} M micellar CTACl solutions, respectively. In these cases, not shown in Figure 1, good linearity was maintained on both sides of the pK_a discontinuity, and the form of the profiles was analogous to that of **8**-OH in Figure 1. As an independent check, the pK_a of 1×10^{-2} M **10**-OH was directly measured as 7.75 by pH titration with 0.5 M NaOH in 3×10^{-3} M aqueous CTACl containing 2.0 vol % DMF at 25 ± 0.5 °C. A Brinkmann 636 "Titroprocessor" automatic titrimeter was used, and the pK_a was read directly from the "half end point" of the classical titration curve. Agreement with the pK_a determined by the kinetic method (7.78) is excellent.

(12) Thiele, J.; Peter, W. *Justus Liebigs Ann. Chem.* **1909**, *369*, 119.
(13) Thiele, J.; Peter, W. *Chem. Ber.* **1905**, *38*, 2842.

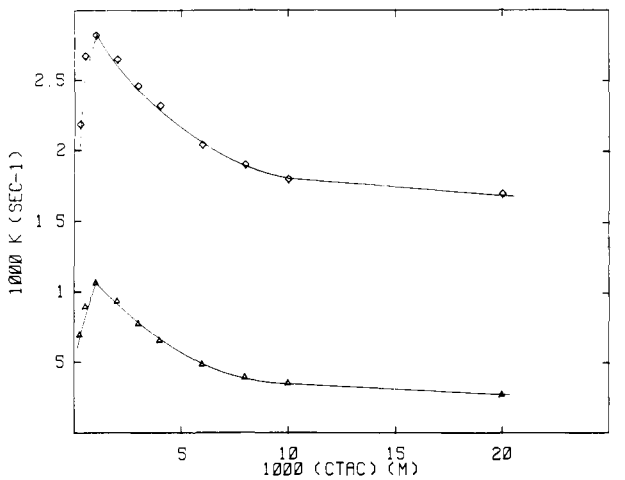

Figure 3. Pseudo-first-order rate constants (k_ψ, s^{-1}) for the cleavages of 1×10^{-5} M PNPDPP by 1×10^{-4} M **8** (◇) or 1×10^{-4} M **7** (△) as a function of [CTACl] at pH 8.0 (**8**) or pH 10.0 (**7**). See text for other conditions and Table I for k_ψ^{max} values.

In contrast to the readily detectable ionizations of **8**-OH–**10**-OH, NaOH titration of 1×10^{-2} M **7**-OH in 1×10^{-3} M aqueous CTACl solution containing 2.0 vol % DMF revealed *no* end point below pH 11.5. The pH–rate constant profile (Figure 2) markedly differed from those of **8**-OH–**10**-OH, as exemplified by **8**-OH in Figure 1. With **7**-OH, there was no evidence (Figure 2) for a discontinuity in the plot of pH vs log K_ψ caused by ionization. The apparent break at pH ~9.4 is associated with the phosphate to borate buffer change at pH 9.0; the same effect is seen in **7**-OH/CTACl and in CTACl alone. We may conclude from Figure 2 that the pK_a of **7**-OH exceeds 11.

Kinetic Studies. The catalytic properties of **7–10** were examined by determining full rate constant–[surfactant] profiles for the cleavage of 1×10^{-5} M PNPDPP by 1×10^{-4} M catayst (**7**-OH–**10**-OH) is varying concentrations of CTACl at 25 ± 0.5 °C. With **7**-OH, we employed 0.02 M disodium hydrogen phosphate buffer at pH 10.0, μ = 0.08 (NaCl); with the other catalysts we used pH 8.0, 0.02 M monobasic/dibasic phosphate buffer, also at an ionic strength of 0.08. Reaction solutions also contained 1.0 vol % DMF and 0.33 vol % CH_3CN.

Pseudo-first-order rate constants, k_ψ, were determined for PNPDPP cleavage at each [CTACl] by spectroscopically monitoring the release of *p*-nitrophenoxide ion at 400 nm. The resulting k_ψ–[CTACl] profiles appear in Figure 3 (for **7** and **8**) and Figure 4 (for **9** and **10**). The reproducibility of k_ψ was better than ±4% in duplicate runs.

In Table I, we display the observed values of k_ψ^{max} for each catalyst, read from the appropriate profile. Also shown are

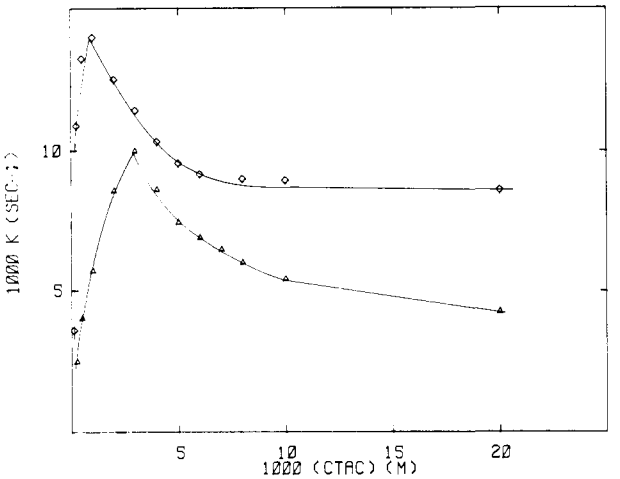

Figure 4. Pseudo-first-order rate constants (k_ψ, s^{-1}) for the cleavages of 1×10^{-5} M PNPDPP by 1×10^{-4} M **9** (◇) or **10** (△) as a function of [CTACl] at pH 8.0. See text for other conditions and Table I for k_ψ^{max} values.

Table I. Kinetic Parameters for Micellar Cleavages of PNPDPP[a]

reagent	10^3[CTACl], M[b]	$10^2 k_\psi^{max}$, s^{-1}	k_{cat}, L/(M·s)[c]
none[d]	1.00	0.018	
1[e]	1.00	6.45	759
7[f]	1.00	0.1	
8	1.00	0.282	44
9	1.00	1.40	179
10	3.00	1.00	160

[a] Conditions (except for **7**): 0.02 M pH 8.0 phosphate buffer, μ = 0.08 (NaCl), 25 ± 0.5 °C, [PNPDPP] = 1.0×10^{-5} M, [reagent] = 1.0×10^{-4} M, 1.0 vol % DMF, 0.33 vol % CH_3CN. [b] Concentration of CTACl at which k_ψ^{max} was observed; see Figures 3 and 4. [c] $k_{cat} = k_\psi^{max}$/[reagent], corrected for 100% ionization to IO^-. See text for pK_a values. [d] No catalyst; see ref 8. This value may be taken as "k_0" in CTACl alone. [e] See ref 3. [f] These results were obtained in pH 10 phosphate buffer; other conditions as in footnote *a*.

Table II. Cleavage of Excess PNPDPP by Reagent **8**-OH[a]

[PNPDPP], M	[CTACl], M	[PNPDPP]/[**8**-OH]	$10^3 k_\psi$, s^{-1}
1.0×10^{-5}	1.0×10^{-3}	1/10	2.81
2.0×10^{-4}	1.0×10^{-3}	2/1	2.03
1.0×10^{-5}	1.0×10^{-2}	1/10	1.80
5.0×10^{-4}	1.0×10^{-2}	5/1	1.73

[a] Conditions as in Table I, footnote *a*; [**8**-OH] = 1.0×10^{-4} M in all cases; other concentrations are as indicated. *p*-Nitrophenoxide ion was followed at 440 nm when [PNPDPP] = 5×10^{-4} M and at 400 nm otherwise.

calculated second-order "catalytic" rate constants ($k_{cat} = k_\psi^{max}$/[catalyst]). These are corrected for 100% I–OH to I–O^- ionizations for **8**-OH–**10**-OH (but not for **7**-OH) on the basis of the pK_a data reported above. Results for *o*-iodosobenzoate, **1**, are included in Table I, so that the last column of the table permits potency comparisons of the various cleavage reagents.

Previous work showed that **1** and its derivatives were true catalysts for the cleavage of PNPDPP in micellar CTACl and that excess substrate could be cleaved with little reduction in the observed values of k_ψ.[2,3,8] In the present study, this point was briefly reinvestigated with **8**-OH; cf. Table II. Again we find kinetic evidence of turnover. Note especially that, with 10^{-2} M micellar CTACl, 1×10^{-4} M **8** cleaved a 5-fold excess of PNPDPP with a rate constant comparable to that measured when the catalyst was in 10-fold excess over substrate. "Burst" kinetics were not observed when the substrate was in excess.

Calculations. We carried out ab initio molecular orbital calculations on the electronic ground states of **10**/**10**-OH and **11**/**11**-OH. Results from the latter pair enabled us to obtain calculated data for **12** and **13**, which were models for the experimentally studied **7** and **8**, respectively. We employed a locally modified and extended version of the GAMESS electronic structure program package.[14] Wave functions for the closed shell singlet states were generated with the standard single determinant restricted Hartree–Fock method of Roothaan.[15a] Bonding and population analyses of the computed wave functions were based on the natural bond orbital (NBO) localization procedures developed by Weinhold et al.[15b]

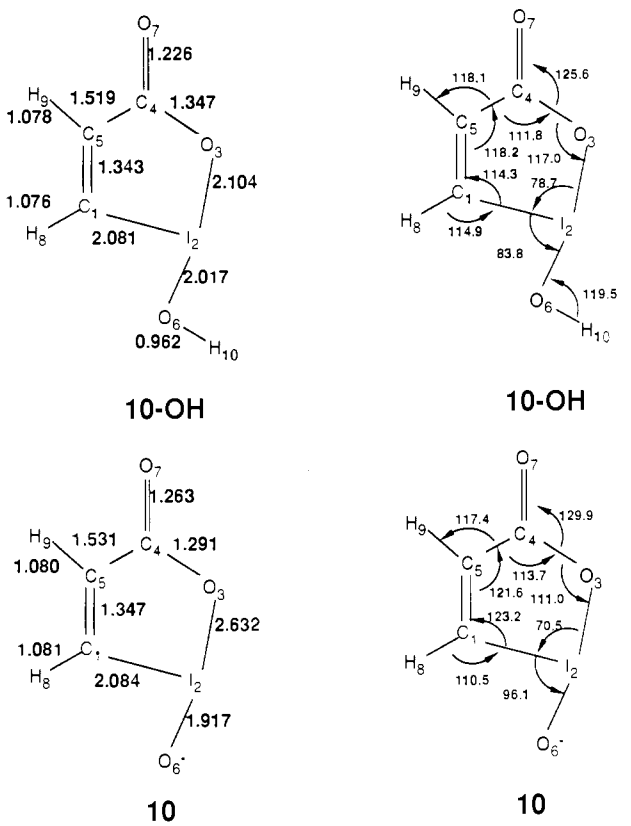

Figure 5. Calculated bond lengths and angles for the conjugate acid–base pair **10**-OH and **10**. See Table III for net atomic charges and π-electron distributions. The calculations are described in the text.

The inner core electrons for I ($1s^2 2s^2 2p^6 3s^2 3p^6 3d^{10} 4s^2 4p^6 4d^{10}$), F ($1s^2$), O ($1s^2$), and C ($1s^2$) were replaced by ab initio effective core potentials (ECPs). We used the relativistic ECP developed by Wadt and Hay[16a] for I and the nonrelativistic ECPs developed by Stevens, Basch, and Krauss for F, O, and C.[16b] The I, F, O, and C valence electrons were described with the basis sets developed specifically for use with these potentials; Huzinaga's minimal basis set (MINI-3) was employed for H.[16c] The I (3s,3p) basis set[16a] was augmented with a set of d functions (exponent = 0.25) and subsequently contracted as follows: (3s,3p,1d)→[2,1/2,1/1]. The valence basis sets for F, O, and C[16b] were split to give a double-ζ type description (4s,4p)→[3,1/3,1]. Geometry optimizations of **10**, **10**-OH, **11**, and **11**-OH (all C_s symmetry) were carried out with these basis sets and ECPs by using Schlegel's scheme,[15c] with analytical gradients and numerical, finite-difference second derivatives. Calculations on **12** and **13** were accomplished by attaching the CH_3 or CF_3 groups with standard[15d] bond lengths and angles to the optimized geometries found for **11** and **11**-OH.

(14) Dupuis, M.; Spangler, D.; Wendoloski, J. *GAMESS*, NRCC Software Catalogue, Vol. 1, Program No. QG01, 1980. Schmidt, M. W.; Boatz, J. A.; Baldridge, K. K.; Koseki, S.; Gordon, M. S.; Elbert, S. T.; Lam, B., private communication. Stevens, W. J.; Krauss, M., private communication.

(15) (a) Roothaan, C. C. J. *Rev. Mod. Phys.* **1951**, *23*, 69. (b) Reed, A. E.; Weinhold, F. *J. Chem. Phys.* **1983**, *78*, 4066. Reed, A. E.; Weinstock, R. B.; Weinhold, F. *J. Chem. Phys.* **1985**, *83*, 735. (c) Schlegel, H. B. *J. Comput. Chem.* **1982**, *3*, 214. (d) Pople, J. A.; Gordon, M. S. *J. Am. Chem. Soc.* **1967**, *89*, 4253.

(16) (a) Wadt, W. R.; Hay, P. J. *J. Chem. Phys.* **1985**, *82*, 284. (b) Stevens, W. J.; Basch, H.; Krauss, M. *J. Chem. Phys.* **1984**, *81*, 6026. (c) Huzinaga, S.; Andzelm, J.; Klobukowski, M.; Radzio-Andzelm, E.; Sakai, Y.; Tatewake, H. *Gaussian Basis Sets for Molecular Calculations*; Elsevier: Amsterdam, 1984.

Table III. Calculated Natural Net Atomic Charges and π-Electron Distributions[a]

	10-OH		10		11-OH		11	
atom	net chg	π-elec	net chg	π-elec	net chg	π-elec	net chg	π-elec
C_1	−0.43	1.07	−0.47	1.07	−0.49	1.13	−0.52	1.11
I_2	1.48	1.96	1.25	1.95	1.44	1.97	1.30	1.96
O_3	−0.94	1.85	−0.94	1.72	−0.98	1.98	−1.07	1.97
C_4	0.94	0.71	0.95	0.70	0.01		0.00	
C_5	−0.27	0.94	−0.29	0.95	−0.18	0.91	−0.20	0.94
O_6	−1.14	2.00	−1.12	1.99	−1.16	2.00	−1.22	1.99
O_7	−0.68	1.47	−0.84	1.60				

[a] See Figures 5 and 6 for the numbering of atoms. See text for details of the calculations.

Table IV. Calculated Ionization Energies for Eq 5

ionization	R	ΔE, kcal/mol
10-OH → **10**	=O	330
11-OH → **11**	H	359
12-OH → **12**	CH_3	363
13-OH → **13**	CF_3	333

Calculated bond lengths and angles for the conjugate acid–base pairs **10**-OH/**10** and **11**-OH/**11** appear in Figures 5 and 6, respectively, whereas, in Table III, we collect net atomic charges and π-electron distributions for these four molecules. The atom numbering schemes of Figures 5 and 6 are employed.

The total energies calculated for **10**–**13** and for each of their conjugate acids permitted the calculation of the energies attending each I–OH → I–O⁻ ionization; cf. eq 5 and Table IV. It will

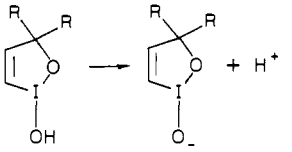

(5)

be noted from Table IV that the calculated ionization energies in the carbonyl and bis(trifluoromethyl) systems (**10** and **13**) are comparable and substantially less endothermic than the analogous ionization processes in the dihydrogen or dimethyl systems (**11** and **12**). The results agree with the ordering of experimentally observed acidities (see above): **1**-OH (pK_a = 7.25) ~ **10**-OH (pK_a = 7.78) ~ **8**-OH (pK_a = 7.75) ≫ **7**-OH (pK_a > 11).

Discussion

Kinetics. The data in Table I indicate that *o*-iodosobenzoate, **1**, retains its pride of place as the most reactive, underivatized oxyiodinane anion yet encountered in the CTACl micellar cleavage of the commonly used simulant substrate PNPDPP. Just as **1** proved to be more reactive than analogues **2**–**6**,[8] it also surpasses the newly tested reagents **7**–**10**.

Reagents **1**, **9**, and **10** are each based on the 1-oxidoiodoxol-3(1*H*)-one system, and their reactivities toward PNPDPP in micellar CTACl are within a factor of 5; i.e., k_{rel}^{cat} **1**:**9**:**10** = 4.7:1.1:1.0. The small advantage of the benzo derivative (**1**) probably stems from a greater hydrophobicity, resulting in stronger binding to the CTACl micelles (where the hydrophobic PNPDPP substrate is also bound) and, consequently, a larger rate enhancement. For example, Lineweaver–Burk analyses[2] of rate constant–[CTACl] profiles for PNPDPP cleavages by **1**[3] and **10** (Figure 4) lead to values of K/N (binding constant/micellar aggregation number) that are considerably larger for **1** (12 500–18 900) than for **10** (1470–2410). (The cmc of CTACl was varied from 1×10^{-4} M to 5×10^{-5} M in these calculations.)

More interesting are the differences between the iodoxolones **1**, **9**, and **10** and the iodoxols **7** and **8**. The 3,3-bis(trifluoromethyl)-1-oxidoiodoxole **8** is ~17 times less reactive than **1**, and its dimethyl analogue, **7**, is still less reactive. There are two factors that affect the nucleophilic reactivities of these reagents. The first is the pK_a of the I–OH form, because it is the I–O⁻ conjugate base that is the reactive nucleophile. The second factor is the intrinsic nucleophilicity of the I–O⁻ anionic form. The unreactivity of "**7**" is clearly due to the low acidity of **7**-OH, with pK_a > 11. This

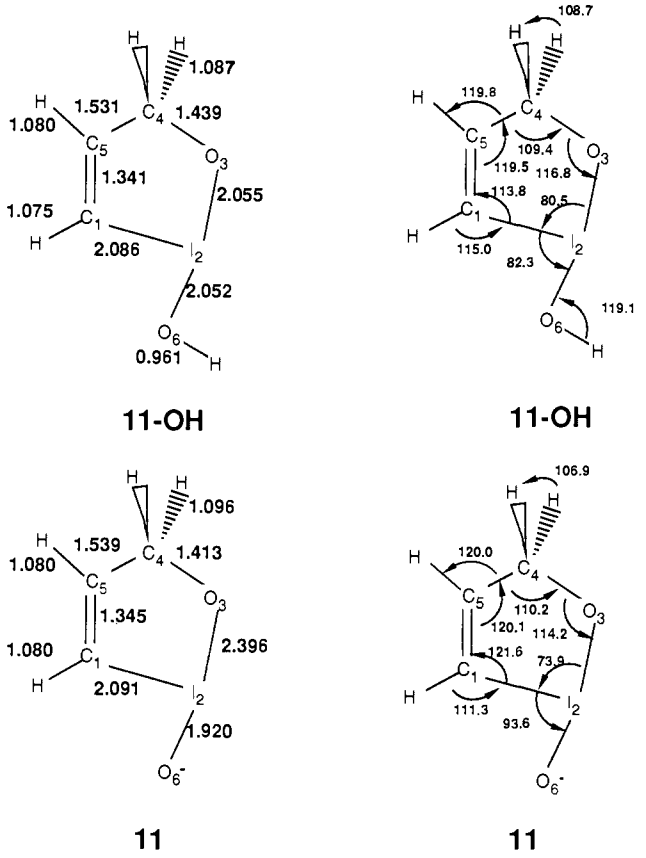

Figure 6. Calculated bond lengths and angles for the conjugate acid–base pair **11**-OH and **11**. Net atomic charges and π-electron distributions appear in Table III.

depressed acidity is clear from experiment (Figure 2) and from the calculated ionization energies (Table IV). Even at pH 10, little conjugate base **7** is present in micellar solutions of **7**-OH, and consequently, there is relatively little enhancement of k_ψ (a factor of ~6) for PNPDPP cleavage, relative to that in micellar CTACl solution alone.

In the case of **8**/**8**-OH, acidity is not a factor. The strong inductively withdrawing CF_3 substituents (σ_I = 0.40[17]) enhance the acidity, and the pK_a of **8**-OH is only 0.5 unit greater than that of **1**-OH. However, the reactivity of **8** toward PNPDPP is 17 times less than that of **1**, on the basis of comparisons of k_{cat}, with correction for pK_a differences (Table I). One's initial impulse is to assert that the CF_3 groups of **8** are more electron withdrawing than the carbonyl group of **1** and that the electron density on the oxido atom of **8** is therefore lower than on the analogous atom of **1**, resulting in a lower nucleophilic reactivity toward PNPDPP. A detailed consideration of our calculations for model systems **10**–**13**, however, shows that the matter is more complicated.

Indeed, given the great interest associated with these (and related[9]) organoiodinanes, it is surprising that there seem to be qualitative[9,18,19] but no quantitative considerations available.

(17) Charton, M. *Prog. Phys. Org. Chem.* **1981**, *13*, 119; cf. p 144.

Accordingly, we now present an appropriately detailed discussion. We will first analyze the optimized geometries of **10**-OH, **10**, **11**-OH, and **11** and then discuss the bonding and charge distributions in these structures, with emphasis placed on **10**-OH and **10**. Finally, we will consider the effects of substituents at C_4.

Geometries. Consider the I–OH compounds **10**-OH and **11**-OH (see Figures 5 and 6). The most striking feature displayed by the optimized structures is the T-shaped coordination geometry around the formally hypervalent iodine atoms.[18,19] Both the internal (C_1–I_2–O_3) and external (C_1–I_2–O_6) angles are near 80° in **10**-OH and **11**-OH. The large deviation from a "regular" pentagon bond angle of 108° in the C_1–I_2–O_3 angle permits the other ring angles to relax to near "ideal" values for their particular coordination, thus diminishing ring strain.[9] The computed I–C and I–O bond lengths in the neutral species are in the 2.0–2.1 Å range, equal to or slightly larger than the sum of their covalent radii (~2.0 Å).[18,20a] As pointed out by a referee, this determines the C_1–O_3 distance as 2.6–2.7 Å, well outside the sum of their van der Waals radii and facilitates the accommodation of the remaining two atoms in the 5-membered ring with little strain. Furthermore, the bond length to the more basic oxygen atom (O_6, the less electronegative of the two O atoms) is the shorter of the two I–O single bond lengths.[18a] These structural features are generally in good numerical agreement with values obtained in X-ray crystallographic studies of closely related compounds.[18a] The bond lengths and angles not involving I_2 are within normal ranges for their types.

The most noticeable divergence between our calculated structures and the crystal structure results is the near equality of the I_2–O_3 (2.10 Å) and I_2–O_6 (2.02 Å) bond lengths calculated for **10**-OH (in the gas phase) compared to 2.30 and 2.00 Å reported for the analogous bond lengths in crystalline **1**-OH.[18a] It is conceivable that intermolecular associations in the crystal between iodine and neighboring lactone carbonyl oxygen atoms[20c] lead to increased inequality of the two I–O bonds.

Substantial geometrical changes around I_2 accompany the deprotonation process at O_6. Consider compound **10**. The asymmetry between O_3 and O_6 increases, and the I–O bond distances become very dissimilar. The computed I_2–O_6 bond length in **10** is 0.10 Å shorter than in **10**-OH, whereas the I_2–O_3 distance increases dramatically by 0.53 Å to more than 2.60 Å. Concomitantly, the C_4–O_3 bond length decreases by 0.05 Å and becomes almost equal to the carbonyl bond length, which increases by an equivalent 0.04 Å. An extreme representation of these changes in **10** is shown in structure **10′**, where the I_2–O_3 bond is

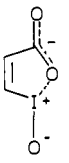

10′

nearly broken, and the O_7–C_4–O_3 unit approaches a carboxylate ion. Curiously, although these changes are strongly reflected in the calculated bond lengths and angles, they are *not* readily apparent in the calculated atomic charges (Table III). Further discussion of this appears below.

There is some direct experimental indication that the carbonyl bond length does increase upon deprotonation of **10**-OH, with a corresponding decrease in the force constant. The FT infrared spectrum of **10**-OH in a KBr pellet shows a peak attributable to the C=O stretch at 1625 cm^{-1}, whereas the corresponding band in the sodium salt of **10** appears at the lower frequency of 1599 cm^{-1}.

At this point one might ask whether structure **10′** implies that ionization of **10**-OH leads to reversion to an iodoso carboxylate tautomer. Several arguments may be advanced against such an interpretation. The I_2–O_6 bond order in **10**-OH is formally 0.5.[18,19] The computed modest reduction (~0.10 Å) in the I_2–O_6 bond length upon deprotonation, and its optimized value in **10** (1.92 Å), which is just below the sum of the covalent radii (~2.0 Å), do not indicate significant double bond character. The bond length for a fully developed I=O bond would be expected to lie in the 1.6 Å range.[20b] Furthermore, there is no intense band in the 650–700 cm^{-1} region corresponding to the I=O stretch[9] in the FTIR spectrum of the sodium salt of **10**. Finally, the large atomic net charges on O_6 and I_2 (Table III) are not readily reconcilable with a covalent I=O description.

In **11**, the decrease in the I_2–O_6 bond length, relative to that of **11**-OH (0.13 Å), is slightly larger than that calculated for the **10**/**10**-OH pair, but the increase in the I_2–O_3 bond length is "only" 0.34 Å, bringing the I_2–O_3 distance to 2.40 Å. There is also a small reduction in the O_3–C_4 bond length of 0.03 Å. The remaining structural variables are virtually unchanged upon ionization of **11**-OH.

Bonding. The bonding in **10**-OH/**10** and **11**-OH/**11** will now be discussed in detail on the basis of results obtained from natural bond orbital (NBO) analysis.[15b] The canonical Hartree–Fock molecular orbitals that form the immediate output of the calculations are very delocalized and difficult to interpret. They do not generally conform to our simple notions of single and double bonds or lone pairs. This is particularly true for the molecules considered here, that have quite unusual bonding features. The NBO procedure allows us to localize a wave function into standard single or multiple bonds, lone pairs, and multicenter orbitals through a series of unitary transformations. The resulting natural bond orbitals describe a single resonance (Lewis) structure and facilitate a direct interpretation of the bonding characteristics. In cases where several choices of electron assignments are conceivable (competing Lewis structures), the "best" set may be deduced on the basis of the total occupancy in bonding and lone pair orbitals versus antibonding and Rydberg orbitals, as well as the magnitudes of the bond orbital interaction energies based on second order perturbation theory analysis of the Fock matrix in the NBO basis set. These criteria also serve as guidance for the overall quality of the localization process.

The best set of localized orbitals from the NBO analysis of **10**-OH describes the overall electronic structure as follows: standard single bonds join C_1–I_2, O_3–C_4, C_4–C_5, O_6–H_{10}, C_1–H_8, and C_5–H_9; standard double bonds exist between C_1–C_5 and C_4–O_7; two lone pairs form on each of the atoms I_2, O_3, O_6, and O_7; and three center–four electron (3c–4e) bonding occurs in the triad O_3–I_2–O_6.[19] The two lone pairs on O_7 are both in the molecular plane, whereas I_2, O_3, and O_6 all have one lone pair in that plane and one perpendicular to it. All bond, 3c, and lone pair orbitals localize well with occupancies of more than 1.95 e in each orbital, except for the in-plane lone pair on O_7 (1.90 e) and the out-of-plane lone pair on O_3 (1.85 e).

Therefore, the electronic structure of **10**-OH is not best represented by a single covalently bonded resonance structure, but must also include a small admixture of ionic components. The result for O_7 indicates strong interaction between its in-plane lone pair and the neighboring C_4–C_5 and C_4–O_3 σ-bonds. The electron deficiency on O_3 partly shows up as a large population (0.20 e) in the C_4–O_7 π^* orbital. There is thus interaction between the 2p(π)-electrons on O_3 and the C_4–O_7 unit that leads to charge polarization and electron transfer toward the carbonyl unit (see also Table III). The in-plane lone pair on O_3 has a large 2s contribution ($sp^{0.9}$ hybridization).

The 3c orbitals consist of a pure 5p orbital from I_2 (only 0.4% 5s and 0.7% 5d character) and hybrid orbitals from O_3 and O_6 that can be described as being of effective $sp^{5.5}$ (λ_1) and $sp^{7.1}$ (λ_2) hybridization, respectively. The fully bonding, in-phase combination of these hybrids (Ψ_1, see illutration) is polarized towards

(18) Reviews: (a) Koser, G. F. In *The Chemistry of Functional Groups, Supplement D*; Patai, S., Rappoport, Z., Eds.; Wiley: New York, 1983; p 721 ff. (b) Nguyen, T. T.; Martin, J. C. In *Comprehensive Heterocyclic Chemistry*; Meth-Cohn, O., Ed.; Pergamon: Oxford, 1984; Vol. 1, p 563 ff.

(19) Musher, J. I. *Angew. Chem., Int. Ed. Engl.* **1969**, *8*, 54 and references therein.

(20) (a) Pauling, L. *The Nature of the Chemical Bond*, 3rd ed.; Cornell University Press: Ithaca, NY, 1960; p 221 ff. (b) Banks, D. F. *Chem. Rev.* **1966**, *66*, 243. Archer, E. M. *Acta Crystallogr.* **1948**, *1*, 64. (c) Etter, M. C. *J. Solid State Chem.* **1976**, *16*, 399.

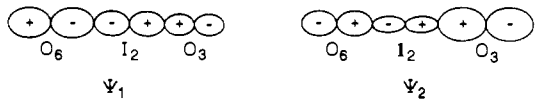

O_6 ($\Psi_1 = 0.79*\lambda_2 + 0.51*5p + 0.35*\lambda_1$, 1.99 e), whereas the "nonbonding" combination (Ψ_2) is fairly localized on O_3 ($\Psi_2 = 0.88*\lambda_1 + 0.11*5p - 0.46*\lambda_2$, 1.88 e). The in-plane lone pair on I_2 is almost solely of 5s character (s^4p hybridization), and the C_1–I_2 σ-bond involves orbitals of sp^4 (I_2) and $sp^{3.6}$ (C_1) hybridization. The implication that the iodine lone pairs in **10**-OH (and also in **11**-OH, see below) reside in essentially localized atomic orbitals rather than in hybrid orbitals accords with a previously offered qualitative bonding model.[18a]

Thus, iodine bonding involves essentially only the 5p orbitals in the σ-system and there is no π-bonding; d orbitals are not important for the description of the iodine atom in **10**-OH or similar systems. Combined with the low electronegativity of iodine, relative to its bonding partners, these factors lead to very strong electron donation from I_2, which consequently acquires a formal positive net charge of 1.48 in **10**-OH (Table III). The oxygen atoms, especially O_3 and O_6, acquire large negative formal charges, but most other atoms in **10**-OH are also indicated to carry large net charges.

The electronic structure of **10** in the conventional σ-system does not differ greatly from that of **10**-OH described above (except that the O_6–H_{10} bond, of course, is no longer present). However, changes take place with respect to the lone pairs, the π-electron distribution, and the three-center bonding around the I atom. The best resonance structure for **10** has three lone pairs on O_6, all with populations larger than 1.95 e and consisting of essentially pure 2s and (two) 2p atomic orbitals. It is in these locallized lone pairs that the strong nucleophilicity of **10** residues. The remaining 2p orbital is engaged in a localized single bond with I_2, in which the effective hybrid orbitals used are $sp^{12.9}$ on O_6 and $sp^{9.8}$ on I_2.

As indicated above, there is virtuallly no covalent bonding between I_2 and O_3, which has two lone pairs in the molecular plane. One of these is a pure 2p orbital (95% 2p character, 1.90 e) directed toward I_2, whereas the other lone pair, as in **10**-OH, has substantial 2s content ($sp^{0.6}$ hybridization, 1.98 e).

The orbitals Ψ_1 and Ψ_2 that are involved in delocalized 3c–4e bonding in the O_3–I_2–O_6 triad of **10**-OH thus localize in **10** into a single I_2–O_6 bond and a lone pair on O_3, representing extreme forms of Ψ_1 and Ψ_2, respectively. Judging from the large atomic net charges, however, there may be polar, stabilizing interactions between O_3 and I_2 in **10** that are represented in **14**. The electronic

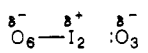

14

configuration around I_2 is completed by two lone pairs, one of the π-type (1.95 e) and one of the σ-type composed mostly of the 5s orbital (1.99 e, $sp^{0.3}$ hybridization), as well as the C_1–I_2 single bond that is formed primarily by p orbitals as in **10**-OH ($sp^{3.2}$ hybridization on C_1, $sp^{5.9}$ on I_2).

There is 3c–4e bonding in **10**, but it occurs in the π-system of the O_3–C_4–O_7 moiety, that resembles a carboxylate group, see above.[21] Inspection of the net number of π-electrons on each atom (Table III) reveals that the only real change in π-populations upon ionization of **10**-OH occurs in the form of a charge transfer of 0.13 e from O_3 to O_7. This is fully consistent with the interpretation of the bonding given above: in **10**-OH we assign essentially a full π-type lone pair to O_3 and a localized, electron-rich π-bond to C_4–O_7, but in **10** we invoke shared 3c–4e bonds for this π-subsystem.

Having discussed the bonding patterns in **10**-OH/**10** in detail, the interpretation of the **11**-OH/**11** pair becomes relatively straightforward. The best description of **11**-OH is clearly made in terms of one C_1–C_5 double bond and single bonds elsewhere, except in the O_3–I_2–O_6 triad. As in **10**-OH, these three atoms each have two lone pairs of electrons and participate in 3c–4e bonding. Again, the fully in-phase combination is mostly I_2–O_6 bonding, whereas the "nonbonding" combination is mostly an O_3 lone pair with slight bonding to I_2. This latter orbital has 1.87 e in it, and it is the only orbital in **11**-OH that localizes with an occupancy less than 1.96 e.

The electronic structure of **11** may be analyzed exactly as that of **11**-OH; i.e., with 3c–4e bonding at O_3–I_2–O_6, where the "nonbonding" combination again localizes poorly (1.88 e). The analysis could also be made as in **10**, where a total of three lone pairs are assigned to O_3, and a formal single bond exists between I_2 and O_6. In this case, the third lone pair on O_3 is directed toward I_2 and localizes poorly (1.85 e). All other orbitals in both species localize well (occupancies above 1.95 e), so that the best description of **11** is in terms of resonance hybrid **15**. The O_3–I_2–O_6 bonding

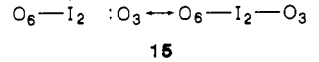

15

in **11** thus represents a case intermediate between **10**-OH/**11**-OH and **10**. This is in line with the computed O_3–I_2 bond length of **11** that is intermediate between the values obtained in **10**-OH/**11**-OH and **10**.

Ionization. The deprotonation of **10**-OH might be expected to lead to considerable alteration in the atomic net charges, but only the charge on I_2 changes noticeably. Several mechanisms operate within **10** to disperse the added charge throughout the entire molecule. About 0.5 e has already been donated from H_{10} to O_6 in **10**-OH that, in combination with the donation from I_2, makes O_6 exceedingly negatively charged (calculated net charge of −1.12 e). The additional 0.5 e "liberated" by the removal of H_{10} migrates into the σ system through the highly polarizable bonds involving O_6–I_2–O_3. Thus, I_2 gains about 0.23 e, O_3 gains 0.13 e, and the remainder (0.16 e) is spread further away into the rest of the ring. The overall charge on O_3 does not change, however, due to the transfer of charge in the π-system to the carbonyl unit to form the carboxylate-type system described above. Although the overall charge on O_6 does not increase upon deprotonation, the additional lone pair and the absence of H_{10} make the accumulated charge readily accessible, effectively increasing the nucleophilicity of O_6 in **10**, relative to that of **10**-OH.

Turning now to the analogous **11**-OH → **11** process, we find first that the acidic H is as positively charged in **11**-OH as it is in **10**-OH. The "extra" one-half electron, as before, goes primarily on I_2 and O_3, but a small amount (0.06 e) actually remains on O_6. We would thus predict that the nucleophilicity of O_6 in **11** would be similar to (or perhaps even exceed) that of O_6 in **10**. However, the energetics of the deprotonation reaction (Table IV), and the pK_a experiments described above, show that the formation of **11** from **11**-OH is far more difficult than the analogous formation of **10**.

The π-distributions in **11**-OH and **11** are virtually identical, because, with the absence of the C_4 carbonyl group, there is no longer a mechanism for moving charge around in the π-system.

Replacement of the two hydrogens on C_4 of **11**-OH with the electron-donating methyl groups (**11**-OH → **12**-OH) makes the ionization process even less favorable. However, the trifluoromethyl groups of **13**-OH facilitate ionization, and catalytic activity is observed in analogue **8**. In **13**, each of the fluorines acquires an additional 0.03 e, relative to their net charge in **13**-OH, for a total $2CF_3$ net withdrawal of 0.18 e, very similar to the effect of the carbonyl group in **10**.

The two oxygens that are common to all the species discussed here (O_3 and O_6) already carry such large negative net charges in the neutral species that they can hardly accomodate any of the additional charge made available upon deprotonation. Thus, it becomes essential to stabilize the generated anion by electron delocalization over as many atoms as possible. Obviously, the carbonyl and trifluoromethyl groups of **1**, **8**, **10**, and **13** have

(21) If we label the 2p(π)-type atomic orbitals on these three atoms as $2p_3$, $2p_4$, and $2p_7$, respectively, then the two delocalized occupied orbitals are described as $0.43*2p_3 + 0.58*2p_4 + 0.70*2p_7$ (occupancy 1.97 e) and $0.82*2p_3 + 0.07*2p_4 - 0.56*2p_7$ (occupancy 2.00 e); i.e., typical bonding and "nonbonding" combinations.

electron-withdrawing capability in common. The hypervalent iodine atom and the 3c–4e bonds act as a shuttle for transferring charge from O_6 into the rest of the molecule, a process that can be facilitated by appropriate substituents at C_4. In addition, the carboxylate feature of **10** may be a particular source of stability, and this extra stability, achieved from π-electron delocalization, may be related to the superiority of catalytic systems derived from **10**-OH.

Conclusions

The nucleophilic properties of several oxidoiodoxoles and oxidoiodoxolones can be rationalized by comparisons of their experimental potencies toward a test substrate and the results of ab initio calculations. A very important conclusion from the calculations is that the "lactone" subunit of the 1-hydroxyiodoxolones acts as a "capacitor", absorbing much of the additional negative charge that accompanies I–OH → I–O$^-$ ionization and simultaneously relaxing toward a "carboxylate". This suggests that appropriately designed structural factors might force the 1-oxidoiodoxolone anions to remain more "closed", thus increasing the negative charge and nucleophilicity at O$^-$ and enhancing reactivity. Experimental tests of this idea are planned.

Experimental Section

General Methods. Melting points and boiling points are uncorrected. NMR spectra were determined on a Varian T-60 or VXR-200 instrument; chemical shifts are reported relative to internal Me_4Si. IR spectra were determined on a Perkin-Elmer 727B spectrometer or on a Mattsun Cygnus 100 FT instrument. TLC analyses were carried out on precoated polyester silica gel plates. Microanalyses were performed by Robertson Laboratory, Florham Park, NJ.

Materials. PNPDPP was prepared and purified by literature methods.[22] CTACl was recrystallized several times from methanol/ether.

1-Hydroxy-1,3-dihydro-3,3-dimethyl-1,2-benziodoxole (7-OH). This compound was prepared as described in Chart I, eq 1. To 0.125 mol of CH_3MgI, prepared in 75 mL of dry ether, was slowly added 15 g (0.057 mol) of methyl *o*-iodobenzoate. The mixture was stirred and refluxed for 1 h and then quenched by addition of saturated aqueous NH_4Cl and crushed ice. The ethereal phase was combined with ethereal extracts (3 × 50 mL) of the aqueous phase and dried over K_2CO_3. Filtration, removal of the ether on a rotary evaporator, and fractionation over a small Vigreux column gave 10.9 g (73%) of (*o*-iodophenyl)dimethylcarbinol: bp 87–92 °C (1 mmHg) [lit. bp 118–121 °C (5 mmHg),[9] 121 °C (5 mmHg)[10]]; ^1H NMR (CCl_4) δ 1.67 (*gem*-Me_2).

Without further purification, the carbinol was converted to the chloroiodoxol by the method of Amey and Martin.[9] To the carbinol (5 g, 19.1 mmol), dissolved in 15 mL of CCl_4, was added 2.2 g (0.020 mmol) of *tert*-butyl hypochlorite. After 10 min of stirring, a yellow precipitate formed. After 30 min, filtration gave a pale yellow solid that was recrystallized from CCl_4 to yield 3.2 g (10.8 mmol, 56.5%) of 1-chloro-1,3-dihydro-3,3-dimethyl-1,2-benziodoxole; mp 148–150 °C (lit.[9] mp 143–145 °C). Spectral properties of the chloroiodoxole have been detailed;[9] the ^1H NMR spectrum of our sample was in agreement with the literature description. The compound gave a single spot on TLC; R_f = 0.78 (1:1 EtOAc/hexane).

The chloroiodoxole (3 g, 10.1 mmol) was dissolved in 45 mL of CH_2Cl_2 and treated with 0.57 g (10.1 mmol) of KOH in 5 mL of water. After 20 min of stirring, the yellow CH_2Cl_2 solution had become colorless. The CH_2Cl_2 phase was removed, dried, over $MgSO_4$, and stripped to give 1-5 g (5.40 mmol, 53%) of the title compound, **7**-OH; mp 140–142 °C (lit.[9] mp 126–128 °C). Our sample of **7**-OH had a ^1H NMR spectrum in agreement with the literature description. It gave a single spot on TLC, R_f = 0.40 (1:1 EtOAc/hexane), and was 99% active for "I=O" in iodometric titration.[11]

Anal. Calcd for $C_9H_{11}O_2I$: C, 38.9; H, 3.99. Found: C, 39.3; H, 3.82.

1-Hydroxy-1,3-dihydro-5-methyl-3,3-bis(trifluoromethyl)-1,2-benziodoxole (8-OH). The preparation of (4-methyl-2-iodophenyl)bis(trifluoromethyl)carbinol[23] and its conversion with *tert*-butyl hypochlorite to 1-chloro-1,3-dihydro-5-methyl-3,3-bis(trifluoromethyl)-1,2-benziodoxole have been described in detail;[9] cf. Chart I, eq 2. Following these procedures, we obtained the indicated chloroiodoxole that was purified by sublimation (75 °C/0.2 mmHg); mp 180–181 °C (lit.[9] mp 179–180 °C). The proton NMR spectrum agreed with the reported one,[9] and the material gave a single spot on TLC, R_f = 0.72 (3:1 hexane/EtOAc).

The slightly yellow chloroiodoxole (2.2 g, 5.3 mmol) was dissolved in 35 mL of CH_2Cl_2 and stirred with 0.3 g (5.3 mmol) of KOH in 5 mL of water; 0.06 g of triethylbenzylammonium chloride was added as a phase-transfer catalyst. After 20 min of stirring at 25 °C, the yellow CH_2Cl_2 solution decolorized. Stirring was continued for an additional 2 h. The CH_2Cl_2 was then separated, dried, and stripped to give 1.8 g of crude **8**-OH, which was dissolved in EtOAc and chromatographed over silica gel with 3:1 hexane/EtOAc as eluent. We obtained 1.5 g (3.75 mmol, 71%) of pure, white **8**-OH: mp 233–235 °C; this material gave a single spot on TLC, R_f = 0.45 (3:1 hexane/EtOAc); ^1H NMR (DMSO-d_6) δ 2.5 (s, 3 H, Me), 3.27 (s, 1 H, OH), 7.5 ("s", 1 H), 7.8 ("s", 2 H, aromatic protons). Iodometric titration[11] revealed >99% "I=O" activity.

Anal. Calcd for $C_{10}H_7F_6O_2I$: C, 30.0; H, 1.76. Found: C, 30.3; H, 2.07.

1-Hydroxy-4-chloroiodoxol-3(1*H*)-one (9-OH). This compound was prepared by modification of the method of Thiele;[12,13] cf. Chart I, eq 3. Acetylenedicarboxylic acid (10 g, 85 mmol) was dissolved in 150 mL of dry ether and stirred with 16 g (99 mmol) of 98% ICl (Aldrich) under nitrogen. The mixture was stirred and irradiated with a sunlamp (which initiated and maintained) reflux for 40 h. The solvent was then removed under vacuum, the solid residue was dissolved in 50 mL of water, and insoluble matter was filtered. The resulting dark brown residue was extracted four times with 50-mL portions of ether, and the combined ethereal extract was washed with aqueous $Na_2S_2O_3$ solution until it was yellow. Finally, the ethereal phase was washed with water, dried over Na_2SO_4, and stripped under vacuum. The resulting yellow solid was dissolved in the minimum quantity of ether, diluted with an equivalent volume of ligroin, and refluxed for 6 h with charcoal. Filtration of the charcoal and removal of the solvent, on a rotary evaporator gave a solid that was leached with hot $CHCl_3$ (to remove the *cis*-iodochloro olefin). The residual solid was dissolved in the minimum quantity of ether. Ligroin was added until a precipitate began to form. The solvent was concentrated under vacuum, and the slightly yellow needles of (*E*)-1-chloro-2-iodofumaric acid were filtered. A second crop was obtained by concentration of the filtrate. A total of 13 g (47 mmol, 55%) of the chloroiodofumaric acid was obtained; mp 228–230 °C dec (lit.[12] mp 200–227 °C).

Next, 7.0 g (25 mmol) of this acid was dissolved in 10.5 mL of water, cooled to 0 °C, and reacted with a slow stream of chlorine gas for 2.5 h. (A yellow precipitate was observed after 40 min.) The yellow, solid product (1,4-dichloro-1,3-dihydro-3-oxoiodoxole-5-carboxylic acid) was filtered, washed with cold water, and dried under vacuum to afford 5.5 g (17.7 mmol, 71%) of crude material; mp 118–120 °C dec (lit.[13] mp 116–120 °C dec).

This was immediately decarboxylated by refluxing 5.0 g (16 mmol) in 5 mL of water. The evolution of CO_2 was observed, and the solution clarified after 10 min. After an additional 10 min at reflux, a white precipitate appeared and refluxing was continued for an additional 15 min. Cooling, filtration, and recrystallization from boiling water gave 2.85 g (11.5 mmol, 72%) of white crystals of **9**-OH: mp 185–187 °C dec (lit.[13] mp 173–183 °C); IR (Fluorolube) 3000, 2400 (OH, br), 1620 (C=O), 1570 (C=C) cm^{-1}; ^1H NMR (DMSO-d_6) δ 8.2 (HC=) (the compound slowly decomposes in DMSO); ^{13}C NMR (DMSO-d_6) δ 120.9 (CH), 122.8 (CCl), 129.5 (C=O). Compound **9**-OH gave >99% activity in iodometric titration.[11]

Anal. Calcd for $C_3H_2O_3ICl$: C, 14.5; H, 0.81; Cl, 14.3. Found: C, 14.5; H, 0.77; Cl, 14.4.

1-Hydroxyiodoxol-3(1*H*)-one (10-OH). This material was prepared by modification of the methods described by Thiele[12] and Boeseker;[24] cf. Chart I, eq 4. Acetylenedicarboxylic acid (10 g, 85 mmol) was stirred with 20 g of 57% aqueous HI (89 mmol) for 1 h, after which a yellow precipitate had formed. The mixture was stirred for an additional 3 h, and then the solid was filtered and dissolved in ~200 mL of ether. The ethereal solution was washed with aqueous $Na_2S_2O_3$ solution and then with water. After drying (Na_2SO_4), the solvent was stripped and the resulting yellow solid was dissolved in the minimum amount of ether. Ligroin was added until precipitation just began. The product was harvested, the solvent was reduced, and a second crop was obtained. In all, we obtained 17.5 g (72 mmol, 85%) of α-iodofumaric acid; mp

(22) Gulick, W. M., Jr.; Geske, D. H. *J. Am. Chem. Soc.* **1966**, *88*, 2928.

(23) We generated anhydrous hexafluoroacetone from 25 g of the trihydrate (Aldrich, 98%) by dehydration with 50 mL of concentrated H_2SO_4. Liberated hexafluoroacetone was passed through a gas washing bottle (H_2SO_4), a column of P_2O_5, and −20 °C trap (for unchanged trihydrate) and was finally condensed at −78 °C. After addition of the trihydrate, the generating flask was heated to 130–140 °C over 3 h to drive over residual hexafluoroacetone. We obtained 10 g (53%) of the anhydrous material.

(24) Boeseken, J.; Schneider, Ch. *Konink Akad. Wetenschap (Amsterdam), Proc. Sci.* **1932**, 1140.

194-195 °C (lit.[12] mp 193-194 °C); ^{1}H NMR (DMSO-d_6) δ 7.55 (vinyl).

Next, 6.0 g (25 mmol) of the iodo acid was dissolved in 6 mL of acetic anhydride, cooled to 0 °C, and treated with 17.6 g 30% peracetic acid (67 mmol) at such a rate that the reaction temperature remained between 0 and 5 °C. After the addition was complete, the reaction was stirred and kept at 0 °C for 5 h. It was then allowed to warm to 25 °C overnight. A white precipitate formed and was filtered, washed with cold water, and dried under vacuum. We thus obtained 3.9 g (15 mmol, 60%) of the crude, white 5-carboxylic acid derivative of **10**-OH; mp 130-132 °C.

Decarboxylation was carried out by adding 3 g (11.6 mmol) of this material to 15 mL of water and by refluxing the mixture. Carbon dioxide was evolved, and after 15 min the solution clarified. The solution was refluxed for an additional 45 min and then cooled to afford a white precipitate. This was filtered and recrystallized twice from hot water to give 1.8 g (8.4 mmol, 72%) of shiny white needles of **10**-OH: mp 156-157 °C; IR (Fluorolube) 2400 (OH), 1630 (C=O), 1580 (C=C) cm^{-1}; ^{1}H NMR (DMSO-d_6) AB quartet centered at δ 7.4, J = 8 Hz (2 vinyl H). This material is unstable after ~5 min in DMSO. It showed >99% iodoso activity on titration.[11]

Anal. Calcd for $C_3H_3O_3I$: C, 16.8; H, 1.41; I, 59.3. Found: C, 16.8; H, 1.30; I, 59.3.

Kinetic Studies. The straightforward equipment and methods have previously been described.[8] Conditions for the determination of pH-rate profiles are described in the text (above), and the profiles for **8**-OH and **7**-OH appear in Figures 1 and 2, respectively. Conditions for the determination of rate constant-[surfactant] profiles are also described above, with the results summarized in Table I and illlustrated in Figures 3 and 4. Reactions of excess PNPDPP with **8**-OH are summarized in Table II. Micellar reactions were generally followed to >90% completion and showed good first-order kinetics (r > 0.999).

Acknowledgment. We are grateful to the U.S. Army Research Office (R.A.M.) and to the National Institutes of Health (K.K.-J.) for financial support. We thank Professor J. C. Martin (Vanderbilt University) for helpful discussions and Professor R. Herber (Rutgers University) for FTIR spectra. Professor L. Romsted provided helpful discussions and access to an automatic titrimeter. Support from the Rutgers University Center for Computer and Information Services is gratefully acknowledged.

Formation of Benzoxathiete under Mild Conditions and Its Valence Tautomerism in Solution to Monothio-*o*-benzoquinone: An Experimental and Quantum Chemical Study

Ali Naghipur,[†] Krzysztof Reszka,[†] Anne-Marie Sapse,[‡] and J. William Lown*,[†]

Contribution from the Department of Chemistry, University of Alberta, Edmonton, Alberta, Canada T6G 2G2, City University of New York, Graduate School, and John Jay College of CUNY and Rockefeller University, 445 West 59 Street, New York, New York 10019.
Received May 2, 1988

Abstract: Aprotic diazotization of 2-[(2-acetoxyethyl)sulfinyl]aniline in dimethoxyethane affords products that include biphenylene and dibenzo-1,4-oxathiane. Detection of these products is consistent with the formation of benzoxathiete and the valence tautomerism to monothio-*o*-benzoquinone with concomitant formation of dehydrobenzene by a competing pathway. The latter was independently trapped with 1,3-diphenylisobenzofuran and with 9,10-dimethylanthracene. The requirement for SO group participation in the formation of benzoxathiete is established by comparison with the behavior of the analogous thioether and sulfone compounds. EPR and spin-trapping experiments confirm the intermediacy of both oxygen- and nitrogen-centered free radicals which is consistent with the homolytic pathways proposed for the diazotization process. Parallel aqueous diazotization of 2-[(2-acetoxyethyl)sulfinyl]aniline affords vinyl acetate, phenol, and halobenzene consistent with the generation of dehydrobenzene but not benzoxathiete under these conditions. Spin-trapping/EPR studies gave no evidence for free-radical components in the protic diazotization reaction. Ab initio calculations using the 3-21G* and 6-31G* basis sets within the Hartree-Fock approximation, as well as the MP2/3-21G* method, predict an energetically feasible tautomerism of benzoxathiete to monothio-*o*-benzoquinone. The 3-21G* calculations reveal the presence of a biradical intermediate for this reaction which, as a singlet, features an energy higher than the benzoxathiete by 33 kcal/mol, while as the corresponding triplet it proves to be lower in energy than the benzoxathiete by 2.5 kcal/mol. This process, however, might be symmetry forbidden. By contrast, the symmetry-allowed [8s + 2s] cycloreversion pathway of benzoxathiete to dehydrobenzene and SO is energetically much less favorable.

1,2-Oxathietanes are novel hetereocycles[1-3] which, while they are of practical and theoretical interest by analogy with the more extensively studied 1,2-dioxetanes,[4] also exhibit unique chemical properties.[1-3] Thus 1,2-oxathietanes, which are isolable at moderate temperatures in organic solvents, undergo characteristic formal [σ2s + σ2a] cycloreversion[5] via a biradical species[6] to thiocarbonyl and carbonyl compounds, as well as the alternative cycloreversion to olefin and SO and, in certain cases, rearrangement via intramolecular oxygen transfer to ring-opened thioether aldehydes.[1-3] The characteristic reactions were found to be sensitive to the nature and extent of substitution. For example, aryl-substituted 2-chloroethyl sulfoxide precursors give rise to competing cyclizations to alternative 1,2-oxathietanes with concomitant vinylogous 1,4-halogen participation.[3]

1,2-Oxathietanes were originally recognized as principal intermediates in the decomposition of anticancer (2-chloroethyl)-sulfinyl nitrosoureas under physiological conditions.[1,2] (2-Halo-

[†] Department of Chemistry, University of Alberta.
[‡] John Jay College of CUNY.

(1) Lown, J. W.; Koganty, R. R. *J. Am. Chem. Soc.* **1983**, *105*, 126.
(2) Lown, J. W.; Koganty, R. R. *J. Am. Chem. Soc.* **1986**, *108*, 3811.
(3) Lown, J. W.; Koganty, R. R.; Naghipur, A. *J. Org. Chem.* **1986**, *51*, 2116.
(4) (a) Richardson, W. H.; Montgomery, F. C.; Yelvington, M. B.; O'Neal, H. E.; *J. Am. Chem. Soc.* **1974**, *76*, 7525. (b) White, E. H.; Wildes, P. D.; Weicko, J.; Dosham, H.; Wei, C. C. *J. Am. Chem. Soc.* **1973**, *95*, 7050. (c) Kopecky, K. R.; Filby, J. E.; Mumford, C.; Lockwood, P. A.; Ding, J. Y. *Can. J. Chem.* **1975**, *53*, 1103. (d) Adam, W. In *Chemical and Biological Generation of Excited States*; Adam, W., Cilento, G., Eds.; Academic: New York, 1982; Chapter 4, and references therein. (e) Turro, N. J.; Lechiken, P. *J. Am. Chem. Soc.* **1972**, *94*, 2886.
(5) Woodward, R. B.; Hoffmann, R. *The Conservation of Orbital Symmetry*; Verlag-Chemie: Weinheim, 1970; p 72.
(6) Naghipur, A.; Lown, J. W.; Jain, D. C.; Sapse, A. M. *Can. J. Chem.*, in press.

0002-7863/89/1511-0258$01.50/0